Received: 23 July 2019 | Accepted: 8 December 2019

DOI: 10.1002/hyp.13684

RESEARCH ARTICLE

WILEY

Seasonal macrophyte growth constrains extent, but improves quality, of cold-water habitat in a spring-fed river

Andrew L. Nichols[1,2] | Robert A. Lusardi[1,3] | Ann D. Willis[1]

[1]Center for Watershed Sciences, University of California Davis, Davis, California

[2]Rochester, New York

[3]Department of Wildlife, Fish, and Conservation Biology, University of California, Davis, Davis, California

Correspondence
Ann D. Willis, Center for Watershed Sciences, University of California Davis, Davis, CA.
Email: awillis@ucdavis.edu

Funding information
The Collins Foundation; California Trout; Collins Foundation; the Nature Conservancy, Grant/Award Number: 04212015-2193

Abstract

Rooted aquatic macrophytes affect abiotic conditions in low-gradient rivers by altering channel hydraulics, consuming biologically available nutrients, controlling sediment transport and deposition, and shading the water surface. Due to seasonal macrophyte growth and senescence, the magnitude of these effects may vary temporally. Seasonal changes in aquatic macrophyte biomass, channel roughness and flow velocity, were quantified and trends were related to spatiotemporal patterns in water temperature in a low-gradient, spring-fed river downstream from high-volume, constant-temperature groundwater springs. Between spring and summer, a nearly threefold increase in macrophyte biomass was positively correlated with channel roughness and inversely related to flow velocity. On average, flow velocity declined by 34% during the study period, and channel roughness increased 63% (from 0.064 to 0.104). During the spring and fall period, the location of a minimum water temperature variability "node" migrated upstream more than 4 km, whereas daily maximum water temperature cooled by 2–3°C. Water temperature modelling shows that the longitudinal extent of cold-water habitat was shortened due to increased channel roughness independent of seasonal surface water diversions. These results suggest that macrophyte growth mediates spatiotemporal patterns of water temperature, constraining available cold-water habitat while simultaneously improving its quality. Understanding complex spatial and temporal dynamics between macrophyte growth and water temperature is critical to developing regulatory standards reflective of naturally occurring variability and has important implications for the management and conservation of cold-water biota.

KEYWORDS

cold-water habitat, hydraulics, macrophytes, spring-fed river, temperature node, water temperature

1 | INTRODUCTION

Climate change affects the availability and extent of cold-water habitat in streams (Isaak & Rieman, 2013). Groundwater-dependent ecosystems near springs and seeps are resilient against projected warming (Kløve et al., 2014; Lusardi, Bogan, Moyle, & Dahlgren, 2016). Spring-fed rivers inherit stable thermal and water quality characteristics of groundwater. When exposed to ambient environmental conditions during downstream travel, diurnal water temperature variability generally increases with distance from spring sources until a pattern of dynamic equilibrium is reached with the river's heat budget (Tague, Farrell, Grant, Lewis, & Rey, 2007; Webb & Zhang, 1999).

However, longitudinal increases in diurnal temperature variability in spring-fed rivers do not always exhibit a monotonic trend (Nichols,

Willis, Jeffres, & Deas, 2014). Often, alternating "antinodes" and "nodes" of maximum and minimum diurnal variation, respectively, develop at predictable downstream locations (Lowney, 2000; Nichols et al., 2014; Polehn & Kinsel, 1997). An initial antinode typically develops 12 hr downstream from a constant-temperature water source, illustrating the temperature difference between parcels of water subjected to either daytime or nighttime thermal energy budgets. After another 12 hr of travel downstream, a temperature node may also develop. This suggests that if meteorological conditions remain constant, a parcel of spring water—regardless of what time it enters a stream—will gain and lose a similar amount of energy over a 24-hr period and generate a temperature time series of minimal variability 1 day's travel time downstream. Downstream antinodes and nodes will continue to develop until meteorological conditions and channel geometry, as opposed to source water temperatures, become the principal determinants of daily water temperature variability (Polehn & Kinsel, 1997). As such, the antinode–node thermal pattern is a useful surrogate to quantify the extent of cold-water habitat influenced by high-volume, groundwater-fed springs. However, the underlying seasonal controls to the longitudinal extent of cold-water habitat are poorly understood.

Dense beds of aquatic macrophytes are often found in low-gradient, spring-fed rivers where stable flow regimes, low stream power, gravel and sand-sized bed materials, limited riparian shading, and nutrient-rich groundwater provide ideal growing conditions (Gurnell, O'Hare, O'Hare, Dunbar, & Scarlett, 2010; Sear, Armitage, & Dawson, 1999). Macrophyte growth patterns affect hydraulic, hydrogeomorphic, and water temperature processes in numerous ways. For example, macrophyte growth typically increases channel resistance to flow (De Doncker et al., 2009; Green, 2005a), progressively reducing flow velocity (Champion & Tanner, 2000) and increasing flow depth per unit volume of discharge (Willis et al., 2017). Patches of aquatic macrophytes also create localized (Green, 2005b) and reach-scale (Nepf, 2012) zones of low velocities bounded by areas of high turbulence, which helps trap mobile bed sediments (Cotton, Wharton, Bass, Heppell, & Wotton, 2006).

More recently, seasonal macrophyte growth has been identified as an important habitat feature associated with juvenile salmonid rearing, due to its various and numerous effects on hydrology, temperature, and prey. For instance, Lusardi, Jeffres, and Moyle (2018) found that macrophytes reduced water velocity and increase prey availability for foraging fishes when compared with other typical bedforms such as gravel, whereas Willis et al. (2017) found that macrophytes, via their canopy, contributed to shading and cooling of stream temperature with important implications for salmonid management. Despite these recent studies, the broader spatial dynamics and effects of macrophytes on hydrology and temperature at the landscape scale and the implications for cold-water biota management, particularly in the face of a changing climate, are relatively unknown. Because dense macrophyte growth tends to occur in streams deemed priorities for cold-water conservation, understanding the feedbacks on the extent and quality of habitat is critical.

The influence of aquatic macrophytes on hydraulic, hydrogeomorphic, biotic, and water temperature dynamics—at both patch and reach scales—suggests that rooted aquatic macrophytes (submerged and emergent) may play a similarly important role controlling the extent and quality of cold-water habitat (Gurnell et al., 2016; Nepf, 2012; Willis et al., 2017). The geographic locations of temperature variability antinodes and nodes are determined by flow velocity (Lowney, 2000). In most rivers, an increase in flow depth with discharge diminishes the effects of boundary resistance, allowing for a direct and positive relationship between flow velocity, depth, and discharge magnitude (Knighton, 1984). Consequently, the distance between successive antinodes and nodes generally increases as discharge magnitude rises and decreases as discharge magnitude falls. However, in streams exhibiting prolific macrophyte growth, seasonal changes in flow resistance (Champion & Tanner, 2000; De Doncker et al., 2009; Nepf, 2012) may alter this relationship, suggesting that seasonal locations of antinodes and nodes may be influenced by velocity reductions associated with macrophyte growth. Although these studies have looked at such relationships independently, the direct feedbacks between aquatic macrophytes, hydrodynamics, and extent of cold-water habitat is not yet quantified.

This study examines whether spring and summer macrophyte growth affects spatiotemporal water temperature patterns in a large spring-fed creek. We hypothesize that progressive seasonal macrophyte growth reduces spring and summertime streamflow velocities and shifts the spatial locations of temperature variability antinodes and nodes upstream, shortening the extent of cold-water habitat. This study is important to understand the seasonal limitations of valuable cold-water habitat, particularly in streams being managed for the recovery and conservation of cold-water species.

2 | MATERIALS AND METHODS

2.1 | Study site

The study was conducted in the Shasta River basin of northern California, USA (Figure 1). A tributary to the Klamath River, the Shasta River is one of the most productive streams available to anadromous fish along the Pacific Coast of northern California and southern Oregon (NRC, 2004). Historically, surface runoff from direct precipitation and snowmelt in the Klamath Mountain's headwaters mixed with voluminous groundwater spring sources, creating a complex hydrologic regime characterized by stable baseflows augmented by seasonal runoff. However, due to upstream water storage and flow regulation (see Null, Deas, & Lund, 2010 for a description of surface water infrastructure in the Shasta River basin), streamflow in the Shasta River below Dwinnell Dam and Lake Shastina is derived predominantly from discrete springs discharging cool (11–13°C) and nutrient-rich groundwater (Dahlgren et al., 2010; Lusardi et al., 2018; Nichols et al., 2014; NRC, 2004). The limited annual precipitation (24–46 cm $year^{-1}$; NCRWQCB, 2006) in the Shasta River basin infiltrates Quaternary basalts and basaltic andesites of the High Cascades bounding the Shasta River to the north and east (Blodgett, Poeschel, & Thornton, 1988; Nathenson, Thompson, & White, 2003), ultimately discharging

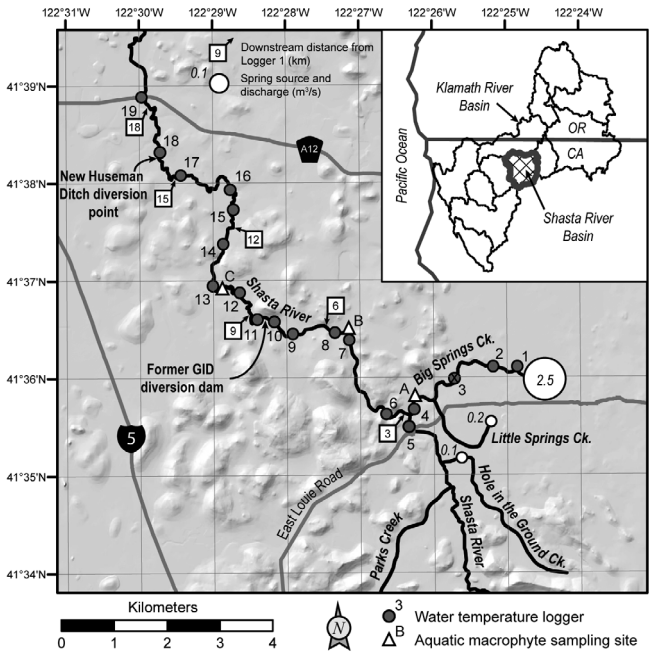

FIGURE 1 Study area in the Shasta River valley of northern California, USA. Water temperatures were continuously monitored at 19 locations along Big Springs Creek and the Shasta River. Aquatic macrophytes were periodically harvested from one location in Big Springs Creek (Site A) and two locations along the Shasta River (Sites B and C). GID = Grenada Irrigation District

downslope at numerous springs along the eastern edge of the Shasta Valley. Principal among these are a group of springs located at the headwaters of the tributary Big Springs Creek (Figure 1). Together, these springs discharge approximately 2.5 $m^3\ s^{-1}$ of streamflow, partially diminished by seasonal irrigation diversions (~0.28 $m^3\ s^{-1}$) and regional groundwater pumping. Spring water travels westward along Big Springs Creek before entering the Shasta River and flowing north towards the Klamath River.

Without the shading effects of riparian vegetation, stable and nutrient-rich streamflow in the low-gradient (mean slope = 0.003), wide, and shallow (mean bankfull width to depth ratio = 84; Nichols et al., 2014) Big Springs Creek promotes extraordinary primary productivity, principally characterized by seasonal growth of native emergent and submerged rooted aquatic macrophytes (Willis et al., 2017). The macrophyte species assemblage in Big Springs Creek is dominated by emergent smartweed (*Polygonum hydropiperoides*) and watercress (*Nasturtium officinale*), as well as submerged northern watermilfoil (*Myriophyllum sibiricum*). The narrower and deeper downstream reaches of the Shasta River (Nichols et al., 2014) also exhibit a complex macrophyte species assemblage dominated by submerged species including pondweed *(Potamogeton pectinatus*) and white water buttercup *(Ranunculus aquatilus*; NCRWQCB, 2006). Macrophyte communities in Big Springs Creek and the Shasta River exhibit pronounced growth and senescence cycles generally characterized by minimum macrophyte biomass in winter and early spring and maximum biomass in late summer and early fall (Willis et al., 2017).

2.2 | Aquatic macrophyte sampling

To quantify seasonal changes in aquatic macrophyte biomass, three locations were sampled downstream from source springs in Big Springs Creek (Sites A, B, and C; see Figure 1). Sampled stream reaches exhibited rectangular channel morphologies with channel slopes ranging from 0.003 m m^{-1} at Site A to 0.001 at Sites B and C. Channel widths ranged from 13 m at Site C to 40 m at Site A. At each site, macrophytes were harvested from six randomly selected sample locations along 100-m stream reaches during March, June, and September 2015. Site C was not sampled during March because water depths were too great to sample. At each location, all above-streambed biomass rooted within a 0.37-m^2 PVC-frame quadrat was removed, and samples were agitated in the stream to reduce the presence of clinging macroinvertebrates and other detrital material. Individual sampling locations were never reoccupied during subsequent sampling periods. Samples were placed in individually labelled bags and returned to the laboratory in ice-filled coolers to prevent decay. In the laboratory, plants were dried at 65°C for ≥72 hr and weighed. Samples were then ashed in a muffle furnace for 4 hr at 475°C, cooled, and reweighed to derive ash-free dry mass (AFDM). Mean standing macrophyte stock from each sampling date was reported as grams AFDM per square metre.

2.3 | Abiotic data

2.3.1 | Water temperature and meteorological data

Water temperature was continuously monitored at 19 monitoring sites along Big Springs Creek (Sites 1 to 4) and the Shasta River (Sites 5 to 19; see Figure 1). Sites 1–4 and 6–16 were monitored using HOBO® Pro v2 (Onset Computer Corporation, Bourne, Massachusetts) water temperature data loggers, programmed to log data every 30 min. Water temperature data from Sites 5 and 17–19 were provided by the Nature Conservancy, also as 30-min time series. Meteorological data were collected from a station located at Site 3. Although loggers were deployed during the March 18 vegetation sampling event, analysis of the temperature data includes the period April 1 through September 30, 2015 to reflect only the full-month portions of the dataset.

2.4 | Velocity, discharge, and roughness

Flow velocity was measured at 0.6 stream depth at 1-m verticals across a repeated channel cross section at each sampling site (A, B, and C; Figure 1) during each seasonal macrophyte sampling event. Velocity in each vertical section was measured using a Marsh McBirney FloMate 2000 electromagnetic velocity metre. Using velocity transect data, wetted cross section area was calculated for each site and sampling period. Discharge magnitude during each macrophyte sampling event was

obtained from either continuous streamflow monitoring stations (Sites A and B) or derived from velocity transect data (Site C) following standard streamflow measurement methods (Rantz, 1982). Mean cross section velocity for each site and sampling period was subsequently derived using the continuity equation (Equation 1),

$$v = \frac{Q}{A}, \tag{1}$$

where v = mean flow velocity (m s^{-1}), Q = discharge (m^3 s^{-1}), and A = wetted cross section area (m^2). To quantify flow resistance at each site and sampling period, Manning's roughness coefficient, n, was calculated using the Manning equation (Equation 2),

$$n = \frac{R^{\left(\frac{2}{3}\right)} S^{\left(\frac{1}{2}\right)}}{v} \tag{2}$$

where R is the hydraulic radius (m), S = channel bed slope, and v = mean flow velocity (m s^{-1}). Hydraulic radius was derived from velocity transect data, channel bed slope was obtained from available longitudinal profile survey data (Nichols et al., 2010), and mean flow velocity data were obtained from Equation 1.

2.5 | Data analyses and analytic validation

For macrophyte biomass, effect sizes were calculated to evaluate seasonal differences in sample means. Cohen's d was calculated by differencing the means of macrophyte biomass samples collected in March and September 2015 and then dividing these means by the pooled standard deviations of the same samples (Cohen, 1988). To examine seasonal trends in aquatic macrophyte biomass, mean flow velocity, and Manning's roughness (n), data were aggregated from all three sampling sites by month (March, June, and September) for each respective variable. Linear mixed effects models were used to test for seasonal differences in biomass, velocity, and roughness between sampling periods. Each model included site as a random effect thus allowing an estimate of the effect of time on the different response variables, while accounting for potential differences between sites. Data were square-root transformed where appropriate to correct for nonnormality and heteroscedasticity and used Shapiro–Wilk tests to confirm normality. Linear regression was used to analyse the relationship between plant biomass, velocity, and roughness. All statistical analyses were performed in R with the lme4 (Bates, Bolker, & Walker, 2014) and nlme (Pinheiro, Bates, DebRoy, & Sarkar, 2014) packages for linear mixed effects models.

To isolate the effect of seasonal macrophyte growth on flow velocity at each monitoring site, roughness coefficients (n) from March 2015 were used to calculate expected June and September streamflow velocities under conditions of unchanging flow resistance using the Manning equation. These velocities were then compared with measured data from the June and September sampling event using percent difference.

To characterize spatiotemporal water temperature trends, first descriptive statistics (mean, median, maximum, minimum, and standard deviation) were calculated for water temperature data across daily and monthly intervals. Using daily maximum water temperature data, monthly trends in the magnitude and standard deviation of maximum water temperatures were characterized at each monitoring location. To determine locations of water temperature variability antinodes and nodes in Big Springs Creek and the Shasta River during each month, water temperature monitoring locations were identified along the studied segment exhibiting maximum and minimum standard deviation of water temperatures, respectively.

A mechanistic water temperature model was used to assess the relationship between water temperature, discharge, and channel roughness changes due to seasonal aquatic macrophyte growth. First, a one-dimensional, steady-flow, numerical water temperature model was used to simulate water temperatures through the study reach, using channel roughness as a calibration parameter. The Water Temperature Transaction Tool (W3T) was developed as an open-access, open-code spreadsheet model to track discrete parcels of water through a stream and evaluate how they influence water temperature over short-term (1–7-day) periods (Watercourse, 2013). Hourly flow and water temperature boundary conditions were applied at all inflows (upstream study boundary and a tributary) and used hourly meteorological data. Hourly records were used to simulate operations of the Grenada Irrigation District diversion pump and used channel roughness to represent aquatic macrophytes.

Two scenarios were simulated to assess the relationship between aquatic macrophyte growth and spatiotemporal water temperature patterns: early season (i.e., June) and late season (i.e., September). Discharge time series were examined to identify 7-day periods when streamflow remained relatively stable during June and September 2015, to coincide with empirical observations of aquatic macrophyte biomass, streamflow, and water temperature. W3T was used to simulate water temperatures during the periods June 20–26 and September 12–18, 2015. To confirm that W3T produced a valid simulation of water temperature dynamics in the study reach, its results were evaluated using performance criteria identified for percent bias, mean absolute error (MAE), and root-mean-squared error (Moriasi et al., 2007). Because W3T tracks parcels of water through a study reach, the results did not share a common time with observed, hourly records at each monitoring site. Thus, W3T model results were evaluated using the weekly average maximum, mean, and minimum water temperatures at 10 sites throughout the study reach. The early season run was selected as the calibration period; the late season run was the validation period.

Once model performance was confirmed, the model was applied to test the role of channel roughness in seasonal node–antinode patterns. First, roughness values for the early season were optimized via calibration. This value was then applied to the late season during validation to confirm the model's ability to accurately represent water temperature processes through the study reach. Finally, the roughness value for the late season was optimized. Roughness values for the

early and late-season periods were optimized using a random effects statistical model (R and the lme4 package) to minimize W3T performance error averaged over 10 monitoring locations throughout the study reach (water temperature monitoring sites 7–16).

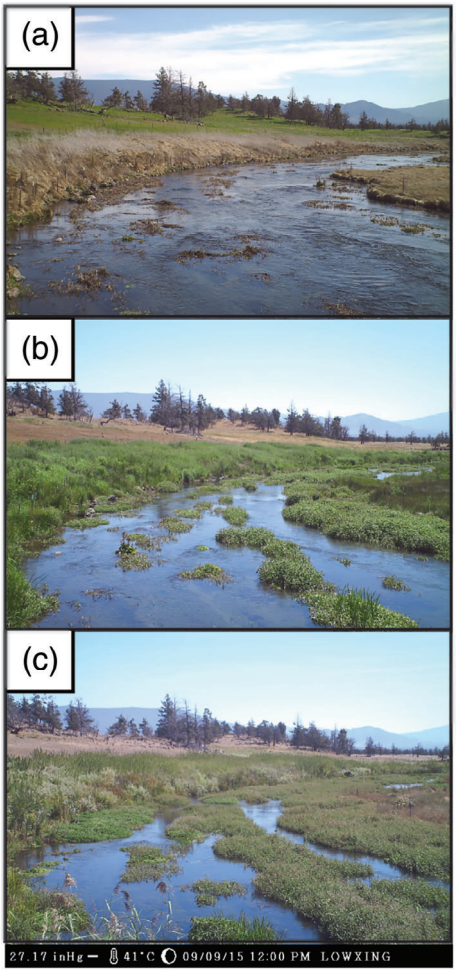

FIGURE 2 Emergent macrophyte growth in Big Springs Creek (Site A) in March (a), June (b), and September (c) 2015

3 | RESULTS

3.1 | Aquatic macrophyte biomass

Qualitative observations identified prolific growth of aquatic macrophytes in Big Springs Creek and the Shasta River between March and September 2015 (Figure 2a–c). Growth patterns at each site were highly variable, generating a "pseudo-braided" channel pattern (sensu Dawson, 1989; Green, 2005b) with dominant flow paths in channel areas free of vegetation. Patches of submerged and emergent macrophytes were observed in Big Springs Creek, with emergent macrophyte patches often extending more than 0.5 m above the water surface during summer (Figure 2c). Submerged macrophytes dominated the species assemblage in the Shasta River downstream from Big Springs Creek. During the sampling period, mean macrophyte biomass over all sites increased from 56.1 grams AFDM per metre in March to 202.8 grams AFDM per metre in September, a 262% increase ($F_{[1,44]}$ = 7.3, p < .01; Figure 3a). An effect size magnitude of 0.64 provided further evidence of positive changes in aquatic macrophyte biomass throughout the 2015 growing season.

3.2 | Channel resistance and flow velocity

Between March and September 2015, average flow velocities decreased from 0.39 to 0.26 m s^{-1} (−34%; $F_{[1,5]}$ = 9.4, p < .05; Figure 3b), whereas mean Manning's n values increased from 0.064 to 0.104 (+63%; $F_{[1,5]}$ = 2.67, p = .16; Figure 3c). Seasonal increases in macrophyte biomass were strongly correlated with decreasing flow velocity (r^2 = .92, p < .001; Figure 4a) and increasing flow resistance (r^2 = .68, p < .01; Figure 4b). Using March 2015 n values as a base roughness coefficient at each sampling site, expected flow velocities were calculated for June and September sampling periods under the assumption of seasonally invariant flow resistance (Table 1). At Sites A and C, predicted flow velocities were up to 241% greater than

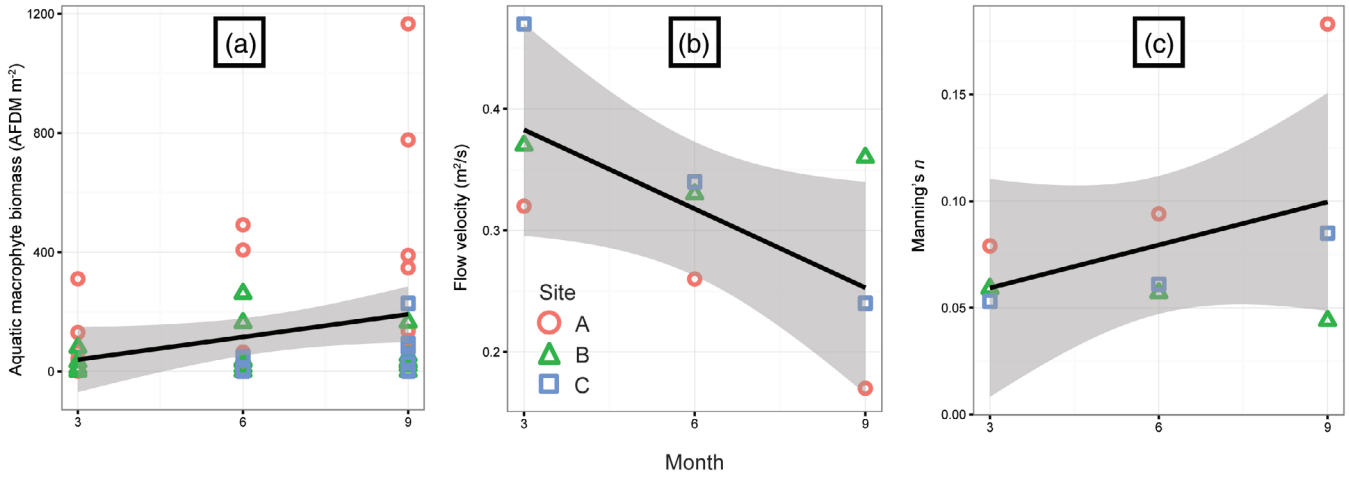

FIGURE 3 Mean changes in (a) biomass, (b) velocity, and (c) Manning's n over the sampling period. Confidence intervals represent ±1 SE

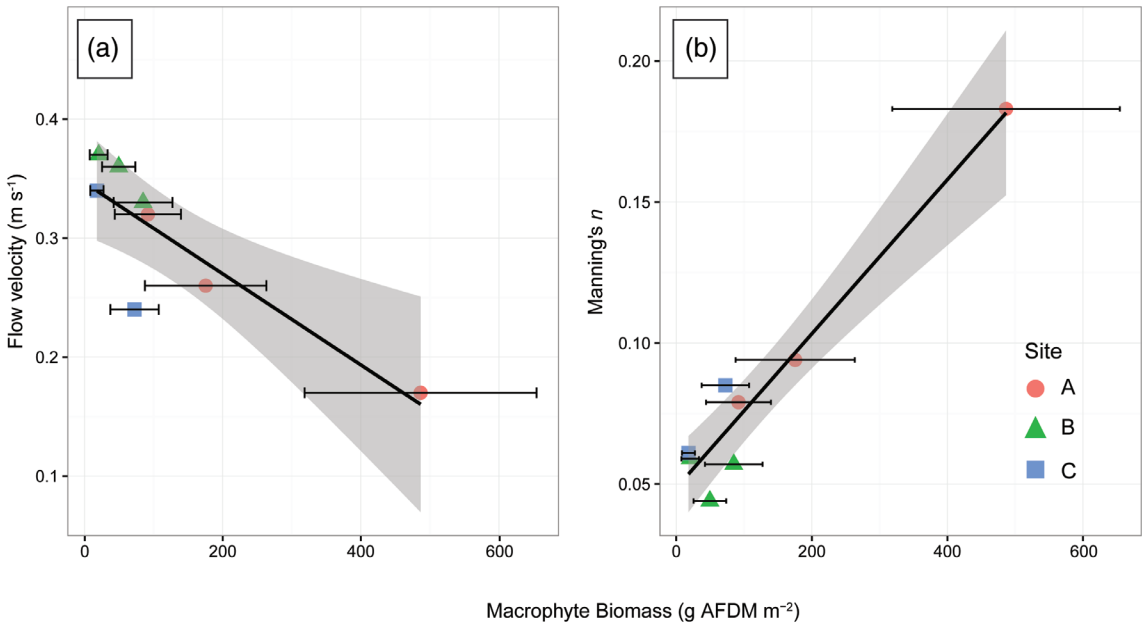

FIGURE 4 Correlations between mean macrophyte biomass (AFDM/m^2) and (a) flow velocity (m s^{-1}) and (b) channel roughness (Manning's *n*). Confidence intervals for biomass represent ±1 SE. AFDM, ash-free dry mass

TABLE 1 Manning's roughness coefficient (*n*) values from March 2015 were used to predict mean flow velocities at sampling sites A, B, and C in June and September 2015 under the assumption of unchanging flow resistance

		Flow velocity (m s^{-1})						
Values of each sampling site		March	June			September		
Site	Manning's *n* (March)	Measured	Measured	Predicted	% diff	Measured	Predicted	% diff
A	0.053	0.32	0.26	0.45	0.73	0.17	0.58	2.41
B	0.059	0.37	0.33	0.31	−0.06	0.36	0.26	−0.28
C	0.053	0.47	0.34	0.39	0.15	0.24	0.38	0.58

observed flow velocities. At Site B, predicted velocities were slightly less than observed flow velocities in both June (−6%) and September (−28%).

3.3 | Water temperature

Rapid daytime warming and night time cooling of source water resulted in progressive downstream increases in water temperature magnitude and variability along Big Springs Creek (Figure 5) resulting in the development of distinct downstream antinodes and nodes. The location of an antinode in Big Springs Creek was consistently observed at or near its confluence with the Shasta River and was spatially stable throughout the study period (Figure 5). The antinode magnitude of variation was greatest during April (σ = 3.1°C) and lowest during August (σ = 1.7°C; Figure 6). A subsequent node was located an additional 12 hr of travel time downstream. Unlike the antinode, however, the location of the node in the Shasta River was spatially unstable. During April and May, water temperature variation in the Shasta River progressively decreased downstream without exhibiting an inflection point between decreasing and increasing variability (Figure 5), implying the presence of a node more than 19 km from the source springs on Big Springs Creek. However, between June and September 2015, the location of this node progressively moved upstream, establishing approximately 15 km downstream from the spring sources in late summer (Figure 5).

Longitudinal variability in the timing of daily maximum water temperatures in Big Springs Creek and the Shasta River accompanied antinode and node development. Daily maximum water temperatures downstream from the source springs occurred progressively throughout the day and into the following night (Figure 7). During spring (April, May, and June), maximum water temperatures at the mouth of Big Springs Creek (Logger 4) occurred at approximately 15:30, whereas daily maximum temperatures in the Shasta River occurred near midnight or extended into the early morning of the following day, approximately 15 km downstream from source springs (Logger 16). During summer (July, August, and September), maximum temperatures at the mouth of Big Springs

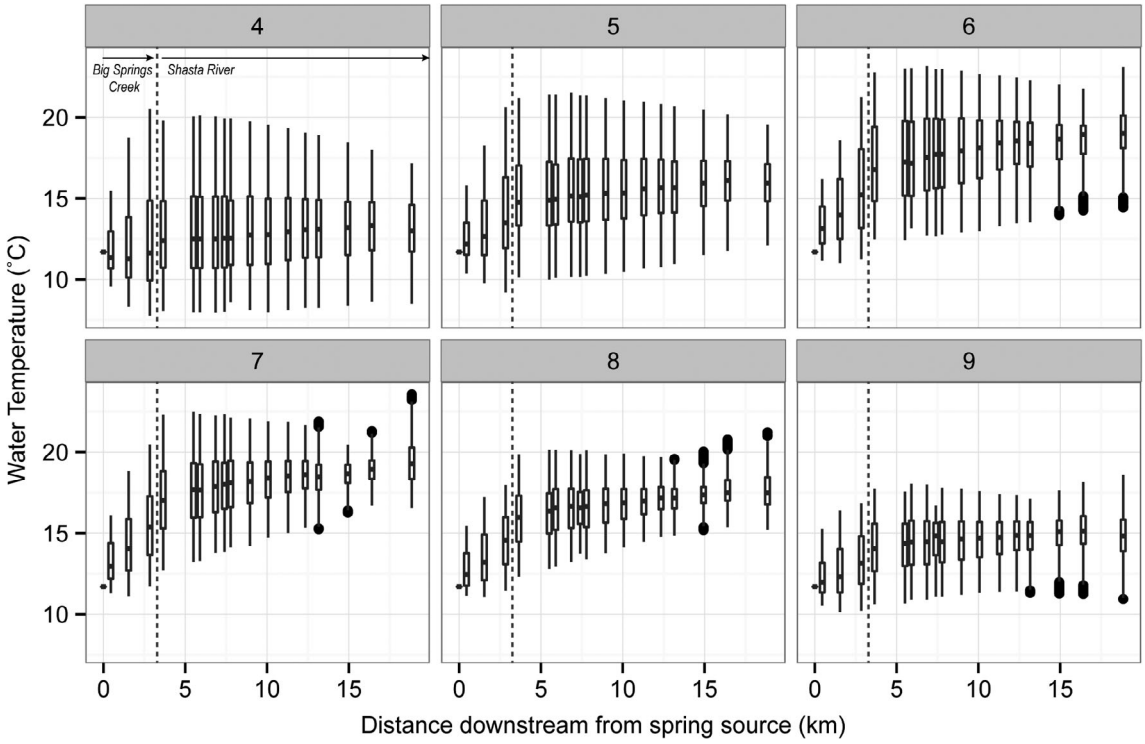

FIGURE 5 Box plots identifying monthly distributions (April through September, 2015) of water temperatures (min, 25th quartile, median, 75th quartile, maximum) at each monitoring location (see Figure 1) extending downstream from the constant temperature spring sources (0 km) to CA County Road A-12 (18.02 km)

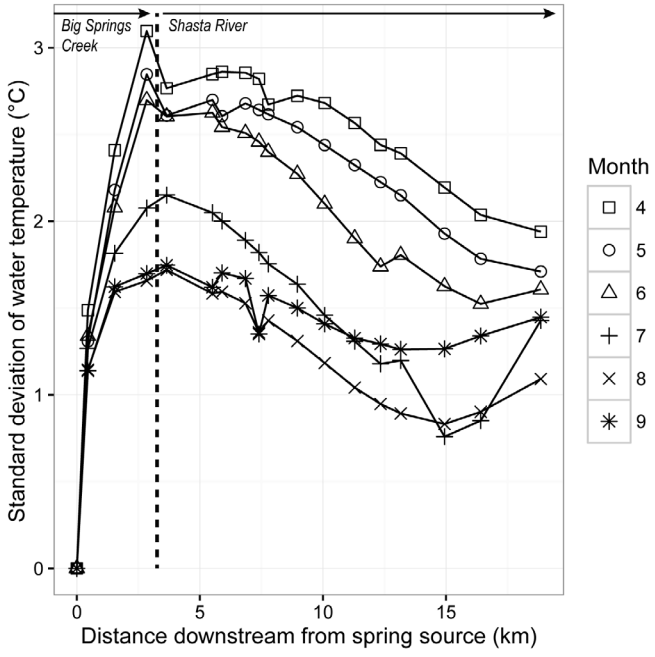

FIGURE 6 Standard deviation of water temperatures measured at each water temperature monitoring location in Big Springs Creek and the Shasta River between March and September 2015

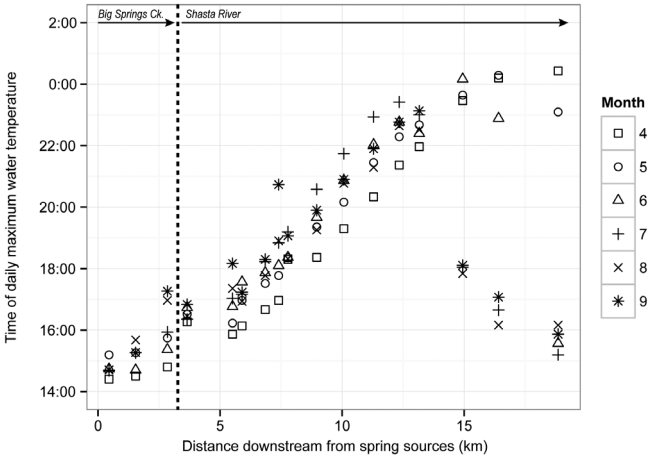

FIGURE 7 Monthly averaged timing of daily maximum water temperatures. The timing of maximum water temperature in the Shasta River downstream from Big Springs Creek is generally out of phase with the timing (i.e., late afternoon) of dominant ambient forcing mechanisms (e.g., solar radiation, air temperature)

Creek occurred at 17:00; a temporal shift is also observed at successive downstream monitoring locations through Logger 15 (23:00) on the Shasta River (Figure 7). However, the timing of daily maximum water temperatures at the summer node (Logger 16) occurred during late afternoon (18:00; Figure 7), presenting an observational departure from upstream loggers. The thermograph at this location exhibited a "multihumped" pattern during August with daily time series exhibiting two peaks (18:00 and 2:00) in between consecutive daily minimums (09:00; Figure 8).

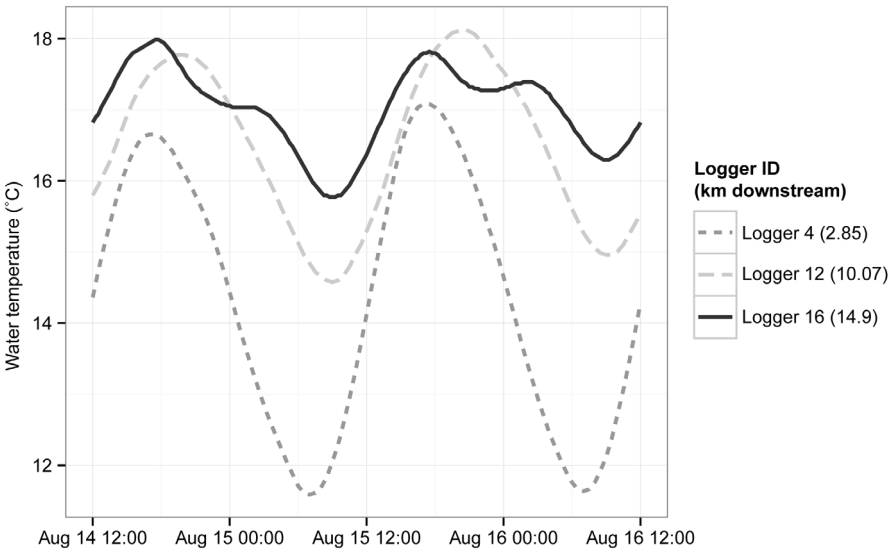

FIGURE 8 Thermographs of water temperature (August 14 to 16, 2015) at locations 2.85 km (Logger 4), 10.07 km (Logger 12) and 14.9 km (Logger 16) downstream from constant temperature spring sources

TABLE 2 Water temperature transaction tool calibration and validation performance results, using weekly maximum, mean, and minimum water temperatures at evaluation metrics

Performance metric, unit	Weekly temperature metric	Early season (calibration)	Late season (validation)
PBIAS, %	Maximum	−0.4	0.8
	Mean	0.3	0.2
	Minimum	0.4	2.4
MAE (0.5*SD), °C	Maximum	0.1 (0.2)	0.2 (0.0)
	Mean	0.1 (0.2)	0.1 (0.1)
	Minimum	0.2 (0.5)	0.3 (0.2)
RMSE (0.5*SD), °C	Maximum	0.0 (0.2)	0.0 (0.0)
	Mean	0.0 (0.2)	0.0 (0.1)
	Minimum	0.1 (0.5)	0.1 (0.2)

Abbreviations: MAE, mean absolute error; PBIAS, performance criteria identified for percent bias; RMSE, root-mean-squared error.

TABLE 3 A summary of the mean reach discharge (Q_m), optimal roughness (n_{opt}), mean depth, and travel time results from the Water Temperature Transaction Tool simulations of early and late season scenarios

Scenario	Period	Q_m (m^3 s^{-1})	n_{opt}	Mean depth (m)	Travel time (hr)
Early season	June 20–27, 2015	2.5	0.075	1.1	6.7
Late season	September 12–18, 2015	2.4	0.080	1.3	7.2

3.4 | Water temperature modelling

Numerical and statistical analyses demonstrated a spatiotemporal relationship between water temperature, discharge, and aquatic macrophyte growth. Modelling results met calibration and validation performance criteria, with the exception of MAE for the validation run (Table 2). However, because the difference between the validation MAE and target MAE were within the margin of error for the data logger accuracy, and because the performance criteria were based on monthly, rather than weekly, analyses, the results satisfied the desired level of performance for this proof of principle application. Performance criteria identified for percent bias was generally <1%, showing a slight tendency to underestimate weekly maximum, mean, and minimum water temperatures. In all cases, MAE was ≤0.3°C, and root-mean-squared error was ≤0.1°C.

Optimized roughness values for the early and late season scenarios showed that the longitudinal extent of cold-water habitat was affected by changes in channel roughness independent of season changes in streamflow. During the early season (June 20–27, 2015), n_{opt} was 0.075 (Table 3), comparable with the average empirical roughness value of 0.074 (Figure 3c). During the late season, n_{opt} increased to 0.080, which was lower than the empirically derived average roughness of 0.104 (Figure 3c). Though mean discharge (Q_m) through the study reach was comparable during the

early and late seasons (2.5 and 2.4 $m^3 s^{-1}$, respectively), mean depth increased from 1.1 to 1.3 m, and travel time increased from 6.7 to 7.2 hr.

4 | DISCUSSION

Seasonal aquatic macrophyte growth is a dominant ecosystem process in numerous spring-fed rivers (Lusardi et al., 2016), broadly affecting the magnitude, variability, and spatial distribution of habitat and water temperature conditions downstream from source groundwater springs. Macrophyte growth throughout spring and summer in Big Springs Creek and the Shasta River structurally shifted the riverine environment by blocking streamflow and shading the water surface. These structural changes induced a series of abiotic responses including increased flow resistance and reduced flow velocity, which interacted to change system hydraulics and dictate spatiotemporal patterns in water temperature. These results suggest that water temperature dynamics in large spring-fed rivers with macrophyte communities are not static, but spatially and temporally dynamic and depend on interactions between macrophyte growth and hydrology.

4.1 | Factors controlling the locations and characteristics of water temperature variability antinodes and nodes

The development of an antinode at the mouth of Big Springs Creek and a node downstream in the Shasta River suggests water temperatures greater than 18 km below the source springs are out of phase with forcing meteorological conditions and do not reach equilibrium temperatures. Consequently, cold-water habitat in this reach reflects the fate and transport of constant-temperature spring water that gradually responds more strongly to ambient meteorological conditions, but initially retains a signature of the constant temperature thermal source.

Contrary to existing field and modelling studies (Khangaonkar & Yang, 2008; Lowney, 2000; Polehn & Kinsel, 1997), the first ("primary") antinode did not occur at the predicted 12-hr travel time downstream from the source springs to Big Springs Creek. Instead, the primary antinode developed at the mouth of Big Springs Creek less than 6 hr of travel time downstream. The consistent geospatial location of this antinode can be attributed to an abrupt change in channel geometry from the wide and shallow Big Springs Creek to the narrower and deeper Shasta River (Nichols et al., 2014). Under the largely steady flow conditions in Big Springs Creek and the Shasta River, this abrupt increase in mean water depth effectively truncates the magnitude and range of observed downstream water temperatures.

Although velocity reductions associated with seasonal macrophyte growth did not affect the location of the water temperature variability antinode at the mouth of Big Springs Creek, the hydraulic and shading effects of progressively emerging macrophytes did influence seasonal patterns of water temperature magnitude and variability at the primary antinode location. As shown by Willis et al. (2017), the effects of macrophyte growth on water temperature patterns in Big Springs Creek can be generally segregated into spring and summer temporal periods. During spring, much of the emergent macrophyte community has yet to emerge above the water surface. During this period, the progressive increase in macrophyte-induced flow resistance creates deeper channel conditions per unit discharge, helping to reduce water temperature variability. Yet, without emergence of macrophyte stems and leaves above the water surface, there is little vegetation to shade the water from incoming shortwave (i.e., solar) radiation—a dominant term in a river's heat budget (Sinokrot & Stefan 1993; Caissie 2006). Consequently, maximum water temperatures at the primary antinode location generally increased throughout spring as thermal loading from solar radiation progressively increased. However, as macrophytes began to emerge through the water surface during summer, water depths continued to increase, whereas the heat flux across the water surface was dramatically reduced due to shading from emerging macrophytes. The net effect of deeper and more shaded conditions along Big Springs Creek was cooler and less variable summertime water temperatures at the antinode location at the mouth of Big Springs Creek.

Although the seasonal growth of aquatic macrophytes and reductions of flow velocities in Big Springs Creek did not affect the location of the primary antinode, macrophyte-induced velocity reductions in the Shasta River forced the location of the primary node to shift upstream during the study period. Throughout spring, the primary node location extended more than 19 km downstream from the spring sources. However, between June and August, during a period of largely stable streamflow, the node migrated upstream more than 4 km, a distance predicted by the approximately 0.10 m s^{-1} reduction in average flow velocities in the Shasta River and Big Springs Creek between June and September 2015.

Temperature modelling results indicate that the spatiotemporal location of the primary node in the Shasta River was influenced by seasonal macrophyte growth-induced reductions in water velocity independent of seasonal streamflow reductions. Numerous field and modelling studies of the fate of constant temperature releases from water supply reservoirs (Khangaonkar & Yang, 2008; Lowney, 2000; Polehn & Kinsel, 1997) indicate that locations of nodes (and antinodes) are principally dependent on water velocity, changes to which are commonly attributed to altered streamflow magnitudes associated with reservoir releases or seasonal streamflow changes. To our knowledge, this is one of the first studies documenting the effects of a seasonal habitat feature influencing the extent of the temperature node location.

With respect to the temperature modelling, differences were observed between optimized (modelled) and empirically derived roughness values in the study (see Tables 1 and 3). These were likely due to differences in the scale and coarseness of the model reach, as well as the uncertainty reflected in the underlying empirical data. For instance, empirical values were determined based on detailed velocity surveys across discrete cross sections, whereas optimized roughness values were calculated as depth- and laterally averaged for an 11-km

longitudinal reach. Thus, the optimized values would have necessarily neglected variations due to macrophyte species, density, and distribution, and natural depth and cross sectional variability, all factors which would influence roughness (Nepf, 2012).

5 | CONCLUSIONS

This study was conducted to quantify the relationship between stream flow, macrophyte growth, and water temperature patterns as they related to the quantity and quality of cold-water, lotic habitat. Degraded thermal conditions in numerous rivers throughout California have contributed to a precipitous decline in salmonid populations (Moyle, Lusardi, Samuel, & Katz, 2017). Macrophytes, common in many spring-fed or partially spring-fed rivers, have recently been recognized as a key salmonid habitat feature because they can strongly and positively influence salmonid prey resources and reduce water velocity, suggesting a bioenergetic advantage for foraging fishes (Lusardi et al., 2018). Macrophytes are also known to affect physical riverine processes including those related to sediment retention, reductions in velocity, accumulation of organic material, and their ability to reduce water temperature as a riverine canopy (Gregg & Rose, 1982; Willis et al., 2017). The influence of macrophytes on thermal conditions at broader spatial scales and potential effects on cold-water biota such as salmonids, however, is less understood.

Our results suggest that macrophytes can play an important role in the spatial and temporal distribution of thermal regimes particularly during the critical oversummer period for cold-water species, such as salmonids. Much of the ecological literature regarding the relationship between salmonids and the magnitude and timing of thermal thresholds is based on research from runoff-dominated ecosystems (e.g., USEPA, 2003). Such thermal thresholds are often spatially explicit and do not consider intrinsic and context-specific processes that may alter the spatial and temporal extent of heating. For instance, on the Shasta River (our study system), Total Maximum Daily Load (TMDL) allocations for water temperature (NCRWQCB, 2006) were established to reduce the effects of elevated thermal regimes on salmonids particularly during the over-summering period. However, these water temperature TMDLs are threshold based (sensu Poole et al., 2004), and do not take into account natural spatial and temporal variability in temperature conditions. Water temperature TMDL compliance standards were also developed under the assumption that late summer (i.e., August) periods of low flow and elevated air temperature created the potential for the highest water temperatures in the Shasta River and greatest threat to thermally sensitive salmonids. However, data presented here and elsewhere (Willis et al., 2017) indicate seasonal macrophyte growth in Big Springs Creek and the Shasta River controls water depths and shading conditions to such an extent that maximum daily water temperatures are typically, and paradoxically, observed in late spring, when day lengths are at seasonal peaks, but water depths and available shade are not yet at seasonal maximums. Late summer daily maximum water temperatures along the study reach are generally 2–3°C cooler than those observed in late spring.

From a regulatory perspective, the development of regime-based water temperature standards (sensu Poole et al., 2004) that account for the spatial and temporal patterns of water temperature described in this paper would help landowners and regulators identify land use or water management actions capable of changing thermal patterns principally controlled by seasonal macrophyte growth. From a river conservation and restoration perspective, minimal macrophyte growth during spring provides the best opportunity to implement projects to reduce water temperatures and/or increase available aquatic habitat for salmonids. Water transfers or other mechanisms used to increase cool streamflow may be most effective during spring, when water temperatures in Big Springs Creek and the Shasta River peak and macrophytes exhibit less control on channel depths and shading conditions relative to summer periods. Conversely, the thermal benefits of increased flows during summer periods are likely to be localized, as the hydraulic and shading effects of macrophytes overwhelm landscape scale thermal response to feasible, small volume (e.g., < 0.25 $m^3 s^{-1}$) water transactions. The recognition of spatial and temporal linkages between macrophyte growth, available aquatic habitat, and water temperature is necessary to develop water management strategies that optimize the extent of cold-water habitat within the natural constraints of an aquatic ecosystem.

ACKNOWLEDGMENTS

We thank the Nature Conservancy for providing access to their property as well as water temperature data. We also thank Drs. Randy Dahlgren, Alex Forrest, Andrew Latimer, and Jon Herman for their invaluable comments and insights regarding a wide range of topics covered in this study. We thank Devon Lambert for his field assistance. We thank two anonymous reviewers for their comments, which considerably improved this manuscript. Funding for this research was provided by the Nature Conservancy and Collins Foundation (grant agreement 04212015-2193), as well as California Trout.

DATA AVAILABILITY STATEMENT

Data available on request from the authors.

ORCID

Ann D. Willis https://orcid.org/0000-0001-9545-2306

REFERENCES

Bates, D., Bolker, B., & Walker, S. (2014). lme4: Linear mixed-effects models using Eigen and S4. *R Package Version*, *1*, 1–7.

Blodgett, J., Poeschel, K., & Thornton, J. L. (1988). A water-resources appraisal of the Mount Shasta area in Northern California, 1985. Retrieved from

Champion, P. D., & Tanner, C. C. (2000). Seasonality of macrophytes and interaction with flow in a New Zealand lowland stream. *Hydrobiologia*, *441*(1), 1–12. https://doi.org/10.1023/a:1017517303221

Cohen, J. (1988). *Statistical power analysis for the Behavioral sciences* (revised ed.). New York, NY: Academic Press, Inc.

Cotton, J., Wharton, G., Bass, J., Heppell, C., & Wotton, R. (2006). The effects of seasonal changes to in-stream vegetation cover on patterns of flow and accumulation of sediment. *Geomorphology*, *77*(3–4), 320–334.

Dahlgren, R., Jeffres, C., Nichols, A., Deas, M., Willis, A., & Mount, J. (2010). *Geologic sources of nutrients for aquatic ecosystems*. Paper presented at the AGU Fall Meeting Abstracts. San Francisco: American Geophysical Union.

Dawson, F. (1989). *Ecology and management of water plants in lowland streams*. Ambleside, UK: Freshwater Biological Association.

De Doncker, L., Troch, P., Verhoeven, R., Bal, K., Desmet, N., & Meire, P. (2009). Relation between resistance characteristics due to aquatic weed growth and the hydraulic capacity of the river Aa. *River Research and Applications*, *25*(10), 1287–1303. https://doi.org/10.1002/rra.1240

Green, J. C. (2005a). Modelling flow resistance in vegetated streams: Review and development of new theory. *Hydrological Processes*, *19*(6), 1245–1259. https://doi.org/10.1002/hyp.5564

Green, J. C. (2005b). Velocity and turbulence distribution around lotic macrophytes. *Aquatic Ecology*, *39*(1), 01–10. https://doi.org/10.1007/s10452-004-1913-0

Gregg, W. W., & Rose, F. L. (1982). The effects of aquatic macrophytes on the stream microenvironment. *Aquatic Botany*, *14*, 309–324.

Gurnell, A., Corenblit, D., García de Jalón, D., González del Tánago, M., Grabowski, R., O'hare, M., & Szewczyk, M. (2016). A conceptual model of vegetation–hydrogeomorphology interactions within river corridors. *River Research and Applications*, *32*(2), 142–163.

Gurnell, A., O'Hare, J., O'Hare, M., Dunbar, M., & Scarlett, P. (2010). An exploration of associations between assemblages of aquatic plant morphotypes and channel geomorphological properties within British rivers. *Geomorphology*, *116*(1), 135–144. https://doi.org/10.1016/j.geomorph.2009.10.014

Isaak, D. J., & Rieman, B. E. (2013). Stream isotherm shifts from climate change and implications for distributions of ectothermic organisms. *Global Change Biology*, *19*(3), 742–751. https://doi.org/10.1111/gcb.12073

Khangaonkar, T., & Yang, Z. (2008). Dynamic response of stream temperatures to boundary and inflow perturbation due to reservoir operations. *River Research and Applications*, *24*(4), 420–433.

Kløve, B., Ala-Aho, P., Bertrand, G., Gurdak, J. J., Kupfersberger, H., Kværner, J., … Rossi, P. (2014). Climate change impacts on groundwater and dependent ecosystems. *Journal of Hydrology*, *518*, 250–266.

Knighton, D. (1984). *Fluvial forms and processes*. New York: Edward Arnold. *Inc*.

Lowney, C. L. (2000). Stream temperature variation in regulated rivers: Evidence for a spatial pattern in daily minimum and maximum magnitudes. *Water Resources Research*, *36*(10), 2947–2955.

Lusardi, R. A., Bogan, M. T., Moyle, P. B., & Dahlgren, R. A. (2016). Environment shapes invertebrate assemblage structure differences between volcanic spring-fed and runoff rivers in northern California. *Freshwater Science*, *35*(3), 1010–1022.

Lusardi, R. A., Jeffres, C. A., & Moyle, P. B. (2018). Stream macrophytes increase invertebrate production and fish habitat utilization in a California stream. *River Research and Applications*, *34*(8):1003–1012.

Moriasi, D. N., Arnold, J. G., Van Liew, M. W., Bingner, R. L., Harmel, R. D., & Veith, T. L. (2007). Model evaluation guidelines for systematic quantification of accuracy in watershed simulations. *Transactions of the ASABE*, *50*(3), 885–900.

Moyle, P. B., Lusardi, R. A., Samuel, P., & Katz, J. (2017). State of the Salmonids: Status of California's Emblematic Fishes 2017. Retrieved from

Nathenson, M., Thompson, J., & White, L. (2003). Slightly thermal springs and non-thermal springs at Mount Shasta, California: Chemistry and recharge elevations. *Journal of Volcanology and Geothermal Research*, *121*(1–2), 137–153.

NCRWQCB. (2006). Staff Report for the ACtion Plan for the Shasta River Watershed Temperature and Dissolved Oxygen Total Maximum Daily Loads. Retrieved from https://www.waterboards.ca.gov/northcoast/water_issues/programs/tmdls/shasta_river/staff_report/.

Nepf, H. M. (2012). Hydrodynamics of vegetated channels. *Journal of Hydraulic Research*, *50*(3), 262–279. https://doi.org/10.1080/00221686.2012.696559

Nichols, A. L., Jeffres, C. A., Willis, A. D., Corline, N. J., King, A. M., Lusardi, R. A. … Moyle, P. B. (2010). Longitudinal Baseline Assessment of Salmonid Habitat Characteristics of the Shasta River, March to September, 2008. Retrieved from https://watershed.ucdavis.edu/pdf/Jeffres-et-al-Shasta-Longitudinal-Baseline-2010.pdf

Nichols, A. L., Willis, A. D., Jeffres, C. A., & Deas, M. L. (2014). Water temperature patterns below large groundwater springs: Management implications for coho salmon in the Shasta River, California. *River Research and Applications*, *30*(4), 442–455. https://doi.org/10.1002/rra.2655

NRC. (2004). *Endangered and threatened fishes in the Klamath River basin: Causes of decline and strategies for recovery*. National Academies Press.

Null, S. E., Deas, M. L., & Lund, J. R. (2010). Flow and water temperature simulation for habitat restoration in the Shasta River, California. *River Research and Applications*, *26*, 663–681. https://doi.org/10.1002/rra.1288

Pinheiro, J., Bates, D., DebRoy, S., & Sarkar, D. (2014). R Core Team (2014) *nlme: linear and nonlinear mixed effects models*. R package version 3.1-118. R Foundation for Statistical Computing, Vienna.

Polehn, R., & Kinsel, W. (1997). Transient temperature solution for stream flow from a controlled temperature source. *Water Resources Research*, *33*(1), 261–265.

Poole, G. C., Dunham, J. B., Keenan, D. M., Sauter, S. T., McCullough, D. A., Mebane, C., … Sturdevant, D. J. (2004). The case for regime-based water quality standards. *Bioscience*, *54*(2), 155–161. https://doi.org/10.1641/0006-3568(2004)054[0155:tcfrwq]2.0.co;2

Rantz, S. E. (1982). Measurement and computation of streamflow: volume 1. measurement of stage and discharge, Geological survey water-supply paper 2175.

Sear, D., Armitage, P., & Dawson, F. (1999). Groundwater dominated rivers. *Hydrological Processes*, *13*(3), 255–276.

Tague, C., Farrell, M., Grant, G., Lewis, S., & Rey, S. (2007). Hydrogeologic controls on summer stream temperatures in the McKenzie River basin, Oregon. *Hydrological Processes*, *21*(24), 3288–3300. https://doi.org/10.1002/hyp.6538

USEPA. (2003). *EPA region 10 guidance for Pacific northwest state and tribal temperature water quality standards*. (EPA 910-B-03-002). Seattle, WA Retrieved from https://www3.epa.gov/region10/pdf/water/final_temperature_guidance_2003.pdf.

Watercourse. (2013). *Water temperature transaction tool (W3T): Technical and user's guide*. Davis, CA: Watercourse Engineering, Inc.

Webb, B., & Zhang, Y. (1999). Water temperatures and heat budgets in Dorset chalk water courses. *Hydrological Processes*, *13*(3), 309–321.

Willis, A. D., Nichols, A. L., Holmes, E. J., Jeffres, C. A., Fowler, A. C., Babcock, C. A., & Deas, M. L. (2017). Seasonal aquatic macrophytes reduce water temperatures via a riverine canopy in a spring-fed stream. *Freshwater Science*, *36*(3), 508–522. https://doi.org/10.1086/693000

How to cite this article: Nichols AL, Lusardi RA, Willis AD. Seasonal macrophyte growth constrains extent, but improves quality, of cold-water habitat in a spring-fed river. *Hydrological Processes*. 2019;1–11. https://doi.org/10.1002/hyp.13684